# *'Mash-up'* design of a high-affinity peptide to highjack microtubule-based transport

Jessica A. Cross[1,2], Magda S. Chegkazi[3], Roberto A. Steiner[3,*], Derek N. Woolfson[1,2,4,*] and Mark P. Dodding[2,*]

[1]School of Chemistry, University of Bristol, Cantock's Close, Bristol BS8 1TS, UK

[2]School of Biochemistry, Faculty of Life Sciences, University of Bristol, University Walk, BS8 1TD, UK

[3]Randall Centre of Cell and Molecular Biophysics, Faculty of Life Sciences and Medicine, King's College London, London, UK

[4]Bristol BioDesign Institute, University of Bristol, Life Sciences Building, Tyndall Avenue, Bristol BS8 1TQ, UK

* To whom correspondance should be addressed:

roberto.steiner@bristol.ac.uk; d.n.woolfson@bristol.ac.uk; mark.dodding@bristol.ac.uk;

## ABSTRACT

Technologies that manipulate and augment the transport of vesicles and organelles by motor proteins along microtubules offer routes to new research tools and therapeutics. Many cargoes for the kinesin-1 family of microtubule motors utilize adaptor proteins that harbor linear peptide motifs that are recognized by the tetratricopeptide repeats of kinesin light chains ($KLC^{TPR}$s). These motifs bind with micromolar affinities at independent but overlapping sites. Here, we employ a fragment-linking peptide design strategy to generate an extended synthetic ligand (KinTag) with low nanomolar affinity for $KLC^{TPR}$s. The X-ray crystal structure of the $KLC^{TPR}$:KinTag complex demonstrates interactions as designed. Moreover, KinTag functions in cells to promote the transport of lysosomes with a high efficiency that correlates with its enhanced affinity. Together, these data demonstrate a new strategy for peptide design to target protein-protein interactions, and its application to hijack endogenous intracellular transport machinery to direct cargo movement within cells.

## INTRODUCTION

Up to 40% of protein-protein interactions (PPIs) are thought to be directed by the recognition of short linear peptides by larger protein domains.[1,2] A subset of these PPIs occur through the recognition of linear motifs by α-solenoid architectures such as tetratricopeptide repeat (TPR) domains, armadillo repeat proteins (ArmRPs) and HEAT proteins.[3,4] In these proteins, tandem arrays of α-helices are stacked together to form extended superhelical structures. This arrangement results in high surface-area-to-volume ratios compared with typical globular proteins and, thus, larger binding surfaces.[5] These domains are important for a diverse range of PPIs in the cell including cell-cycle regulation, chaperone activity, transcription, protein translocation and intracellular transport.[6] It is becoming clear that these interactions are amenable to design, engineering and chemical manipulation, making them potential therapeutic targets for a range of diseases.[7-9]

Kinesin-1 is a ubiquitous microtubule-dependent molecular motor that plays a key role in the spatial and temporal organisation of the cell through transport along microtubules of a diverse range of cargoes including protein complexes, membrane-bound organelles, bacteria and viruses.[10-14] This activity is particularly important in the neuronal axon, explaining why dysregulation of transport can contribute to neuron pathogenesis and is associated with neurodegeneration, including Alzheimer's disease.[12] Thus, understanding the mechanisms by which kinesin-1 interacts with its cargo is important to gain insights into the normal and pathological roles it plays in intracellular transport. In addition, developing reagents to hijack this endogenous motor protein could provide new tools to understand the molecular basis of these processes, and may present routes to new classes of therapeutics.

Kinesin-1 is a heterotetramer of two heavy chains (KHCs) and two light chains (KLCs) (Fig. 1a). While KHCs bear the motor domains that are ultimately responsible for the translocation of kinesin-1 on MTs, much of the ability to transport cargoes depends on the recognition of short acidic peptide sequences found within organelle-associated cargo adaptor proteins by TPR domains of the KLCs ($KLC^{TPR}$s).[15-17] Cargo adaptor peptides act as molecular bridges between specific organelles and the cytoskeletal transport system. Some of these have been characterised structurally in complex with their cognate $KLC^{TPR}$ receptor (Fig.1b,c).[17] These include an internal region of the lysosomal cargo adaptor SKIP and peptides from the *C* termini of JIP1 and Torsin A.[15,16]

Previous structural and biochemical work has identified two distinct classes of peptide sequences: tryptophan-acidic (W-acidic) motifs found in SKIP and in many other adaptors feature a tryptophan residue flanked by aspartic or glutamic acids in the consensus L/M-D/E-W-D/E; Y-acidic motifs at the *C* termini of JIP1 and Torsin A display a tyrosine residue flanked by acidic residues. In mammals there are four closely related KLC isoforms (KLC1 – 4). Whilst W-acidic motifs typically bind both KLC1 and KLC2, *C*-terminal Y-acidic motifs bind the TPR domain of KLC1 with a much higher affinity compared to KLC2.[15,16] These motifs bind at distinct yet overlapping locations on the concave surface of the TPR domain. Peptide binding increases the curvature of the solenoid-shaped TPR through an induced-fit mechanism that highlights the adaptive plasticity of this domain as a platform for protein interactions (Figure 1b).[15,16] These natural motor-cargo adaptor interactions have μM affinities *in vitro*. Presumably, tighter interactions are achieved in the cell through avidity, as multiple copies of the adaptor peptides are expressed on the surface of organelles and the kinesin-1 heterotetramer presents a pair of KLCs.[15,16] Several reports also

indicate an important role for co-operative interactions with the KHCs, again generally in the μM range.[18-20] Taken together, these studies support the notion that a network of low-affinity interactions between adaptors and KHC and KLC co-operate to effect cargo recognition. Appending multiple copies of W-acidic sequences in tandem or triplicate enhances the efficiency of transport, which suggests that μM binding is a limiting factor.[21] Thus, increasing cargo adaptor affinity could augment transport.

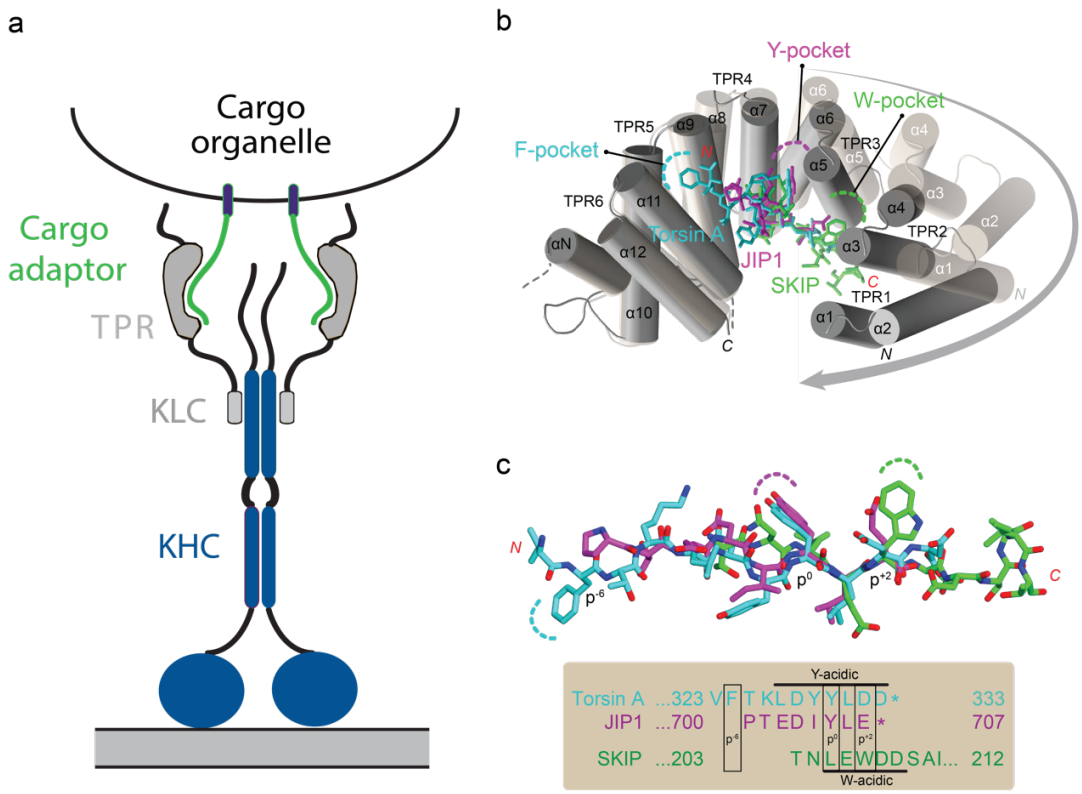


**Fig. 1 | Kinesin-1 and recognition of cargo adaptor peptides. (a)** Schematic of the kinesin-1 tetramer formed by two kinesin heavy chains (KHCs) and two kinesin light chains (KLCs). Cargo adaptor peptides are recognised by the tetratricopeptide repeat (TPR) domains of KLCs ($KLC^{TPR}$s). **(b)** Cartoon representation of the cargo adaptor peptides of SKIP (green sticks, PDB code, 3ZFW), JIP1 (magenta, 6FUZ), and Torsin A (cyan, 6FV0) bound to the concave surface of $KLC^{TPR}$ (solid grey helices). All peptides bind in the direction indicated by the red *N* and *C* letters. The $KLC^{TPR}$ domain is formed of six helix-turn-helix TPR repeats (helices α1 – α12) and an additional non-TPR helix (αN) between TPR 5 and TPR 6. A flexible region between αN and α11 is indicated by the broken line. For simplicity, only one representative peptide-bound $KLC^{TPR}$ is shown. The $KLC^{TPR}$ domain in the peptide-free form (PDB code, 3NF1) is also shown as transparent cylinders with the arrow representing the domain closure elicited by peptide binding. Key binding pockets (F-, Y- and W-pockets) on $KLC^{TPR}$ are highlighted. **(c)** Structure-based sequence alignment of the W-acidic motif of SKIP and the *C*-terminal Y-acidic motifs of JIP1 and Torsin A (asterisk indicates *C* terminus). Their colour code is as in panel **b** with nitrogen and oxygen atoms in blue and red, respectively. The labels $p^{+2}$, $p^0$, and $p^{-6}$ refer to the relative positions of peptide residues buried in the W-, Y-, and F-pockets of $KLC^{TPR}$ with the Y residue of the Y-acidic motif as reference ($p^0$).

Downstream, these adaptor peptide-KLC$^{TPR}$ interactions trigger, or stabilize, larger-scale conformational changes in the kinesin-1 tetrameric motor. This results in a shift from a compact autoinhibited state to a more extended, active form capable of hydrolyzing ATP and generating motile force to transport cargo on the microtubule cytoskeleton.[22-25] One important change is the displacement of an autoinhibitory peptide (LFP-acidic motif) that binds to a KLC$^{TPR}$ site overlapping that for W-acidic peptides. Binding of W-acidic peptides displaces this interaction. Consequently, when targeted to the cytosolic face of an organelle membrane, these particular adaptor sequences are sufficient to drive kinesin-1 dependent transport.[,] In contrast, the binding of the *C*-terminal Y-acidic peptide of JIP1 at the adjacent site does not relieve KLC$^{TPR}$ autoinhibition and requires additional interactions to support efficient transport.[10,16,21,26,27]

Adaptable and synthetically accessible peptides are attractive candidates for disrupting PPIs as they mimic the natural interactions to compete for binding.[28] However, protein-peptide interactions are often dynamic and weak due to the conformational lability of linear peptides. Thus, a challenge is to design peptide ligands that overcome this limitation by making additional or improved interactions with the target.[29,30] Here we describe a structure-guided, fragment-linking approach, which we call '*mash-up'* design, to deliver a high-affinity peptide ligand that targets kinesin-1:cargo interfaces. This combines functional elements of different natural cargo-adaptor sequences into one peptide. Notably, it integrates the transport-activating capacity of W-acidic sequences with the extended binding interfaces from Y-acidic sequences. Our approach borrows from consensus design, which identifies key amino acids for a protein structure from multiple-sequence alignments.[31,32] However, it builds on this by incorporating offset fragments, analogous to fragment-based small-

molecule drug design.[33,34] The *de novo* peptide, which we call KinTag, is effective in hijacking the transport function of endogenous kinesin motors in cells, and can deliver cargo into axons of primary neurons.

## RESULTS

### *Mash-up* design of peptide ligands for KLC TPR domains

The tryptophan and tyrosine residues in W-acidic and Y-acidic motifs, respectively, are essential for binding.[15,35] The X-ray crystal structures of cargo-adaptor peptides from SKIP, JIP1 and Torsin A complexed with $KLC^{TPR}$ domains have identified how these residues interact with their receptor. In the $KLC2^{TPR}$:SKIP complex, the central tryptophan (W, $p^{+2}$ in Fig. 1c) residue occupies a hydrophobic pocket formed between TPRs 2 and 3 (the W-pocket) whilst the Y-acidic tyrosine (Y, $p^{0}$) of both JIP1 and Torsin A bound to $KLC1^{TPR}$ occupies a second pocket formed by repeats 3 and 4 (Y-pocket). The latter can also accommodate leucine or methionine residues often found at this position in W-acidic motifs. For Torsin A, an additional phenylalanine (F, $p^{-6}$) occupies a third pocket (F-pocket) formed by TPRs 5 and 6 (Fig. 1b). Key to peptide stabilization within the concave surface of $KLCs^{TPR}$ is an induced-fit closure of the receptors' solenoid-shaped architecture that enables further hydrogen-bond formation.

A structure-guided overlay of SKIP, JIP1, and Torsin A $KLC^{TPR}$-bound cargo adaptor peptides (Fig. 1c) suggested the possibility of simultaneously engaging the F-, Y- and W-pockets with a single peptide. Therefore, we sought to combine these different features of the natural sequences into a single synthetic-peptide ligand for $KLC^{TPR}$ domains. Our first aim was to produce an extended chimeric peptide with both the transport-activating function of W-acidic peptides and increased binding affinity by incorporating Y-acidic interactions.[33,34] Our overall aim was to deliver a peptide that

out-competes natural peptides to hijack kinesin-1 function in cells. To do this, we used a '*mash-up'* approach to design peptide sequences that extend the *N* terminus of the SKIP W-acidic motif with residues from the JIP1 (J-S peptides), or with residues from both JIP1 and Torsin A (T-J-S peptides). Since the $p^{-2}$ leucine of SKIP and the $p^{0}$ tyrosine from JIP1 and Torsin A bind to the same Y-pocket, two peptides each were designed for each of the J-S and T-J-S constructs (Table 1).[15,16] The designs of these four peptides were made by solid-phase peptide synthesis with the 5-carboxytetramethylrhodamine (TAMRA) fluorophore appended *N* terminally. These were purified by high performance liquid chromatography and confirmed by MALDI-TOF mass spectrometry (Supplementary Fig.1, Supplementary Table 1).

**Table 1 | Sequences and *in vitro* binding affinities of natural and designed cargo adaptor peptides**

| Peptide name | Sequence | $K_D$ KLC1 / nM | $K_D$ KLC2 / nM | $K_D$ KLC1$^{ext}$ / nM | $K_D$ KLC2$^{ext}$ / nM |
|---|---|---|---|---|---|
| *Peptides from natural cargo adaptors* | | | | | |
| SKIP (S) | STNLEWDDSAI | 1170 ± 176 | 1690 ± 132 | 7530 ± 125 | 10650 ± 420 |
| JIP1 (J) | PTEDIYLE | 950 ± 90[16] | - | 2210 ± 60[16] | - |
| Torsin A (T) | TVFTKLDYYLDD | 1720 ± 130 [16] | - | - | - |
| *De novo cargo adaptor peptides from mash-up design* | | | | | |
| J-S(L) | GTEDILEWDDSAI | 1120 ± 153 | 280 ± 94 | 2840 ± 50 | 2570 ± 212 |
| J-S(Y) | GTEDIYEWDDSAI | 430 ± 87 | 210 ± 27 | 960 ± 26 | 2500 ± 82 |
| T-J-S(L) | GTVFTTEDILEWDDSAI | 1200 ± 188 | 657 ± 133 | 1250 ± 110 | 2840 ± 135 |
| T-J-S(Y) '*KinTag*' | GTVFTTEDIYEWDDSAI | 35 ± 7 | 207 ± 15 | 170 ± 7 | 720 ± 29 |

## Synthetic peptides bind KLC$^{TPR}$s *in vitro* with high affinities

The binding affinities of the designed peptides to KLC$^{TPR}$ proteins comprising TPRs 1 – 6 were determined *in vitro* using fluorescence polarization (FP) assays. TAMRA-labelled peptides were incubated with increasing concentrations of KLC$^{TPR}$ proteins in saturation-binding experiments[16] to obtain dissociation constants, $K_D$, for both KLC1$^{TPR}$ and KLC2$^{TPR}$ (Fig. 2, Table 1). The designed peptides had increased affinities over the natural sequences for both isoforms. Peptides J-S(L) and J-S(Y) bound with moderately increased affinities, with the tyrosine variant as the tighter binder. The

lower affinity of the peptides with $p^0$ occupied by L, compared to Y, could be due to the loss of hydrogen bonds in the Y-pocket (Supplementary Fig. 3). Increasing the *N*-terminal extension in the T-J-S(Y) peptide led to a further increase in affinity, but this was not observed for the leucine variant. Thus, peptide T-J-S(Y) had the highest affinities for $KLC^{TPR}$ with $K_D$s of tens of nM to $KLC1^{TPR}$ and hundreds of nM to $KLC2^{TPR}$, Table 1. We dubbed this 'KinTag'.

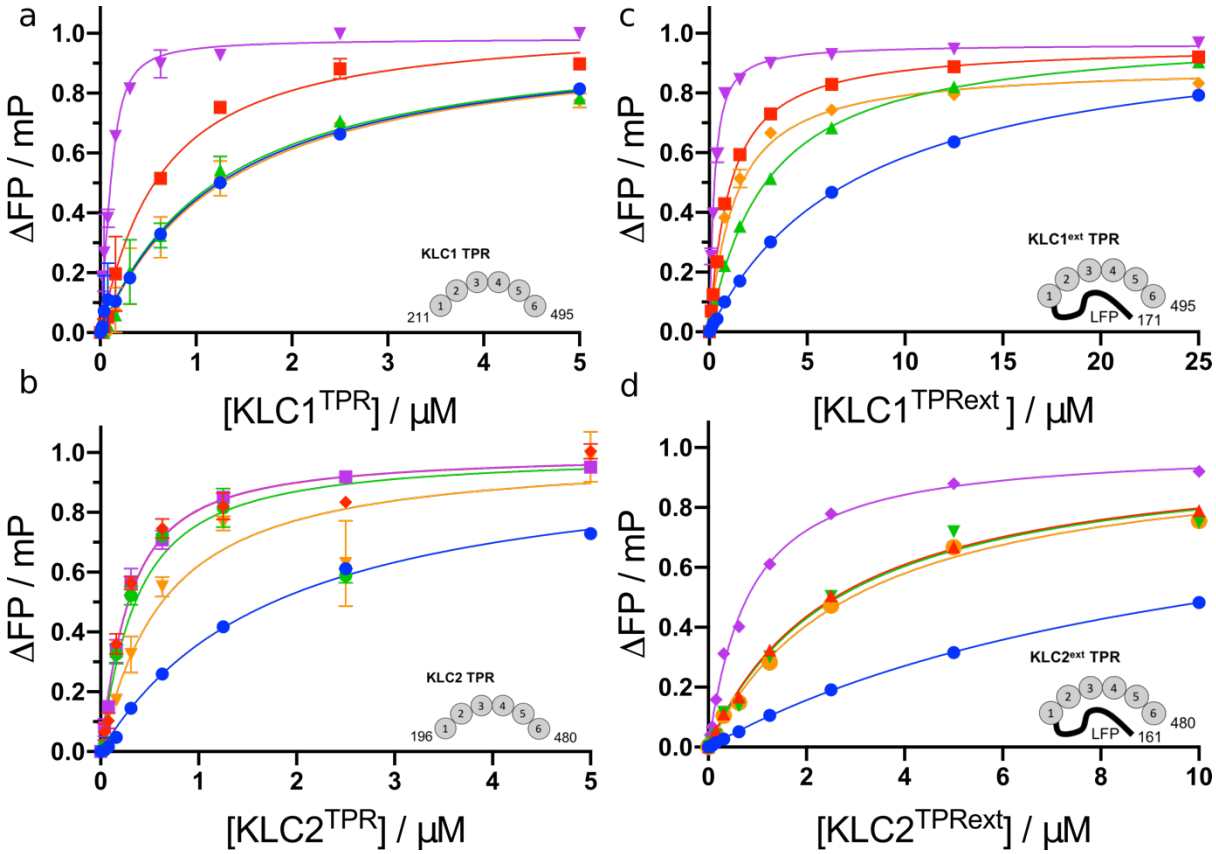


**Fig. 2 | *In vitro* binding affinities of peptides for TPR domains.** Fluorescence polarization assays for TAMRA-labelled peptides (150 nM) incubated with increasing concentrations of protein: **(a)** $KLC1^{TPR}$, **(b)** $KLC2^{TPR}$, **(c)** $KLC1^{TPRext}$, and **(d)** $KLC2^{TPRext}$. Key: natural SKIP, blue; J-S(Y), red; J-S(L), green; T-J-S(L), orange; and T-J-S(Y), KinTag, purple. Data were fitted to single-site binding models with polarization values of the peptide and buffer alone subtracted and values normalised to the calculated $B_{max}$. Error bars indicate 1 SD from a minimum of 3 replicates.

## Designed peptides are sensitive to $KLC^{TPR}$ autoinhibition

KLCs have a conserved autoinhibitory leucine-phenylalanine-proline-containing sequence (LFP-acidic) *N* terminal to their TPR domains. This binds near TPR2 of

KLC$^{TPR}$ and partly overlaps the W-acidic binding region.[22] In FP experiments, the presence of this region reduces the affinity of W-acidic peptides for the TPR domains, but not that of the Y-acidic peptide of JIP1. Consequently, this reduction in binding affinity can be interpreted as a proxy for the capacity to displace the inhibitory interaction.[16,22] Since a functional, transport-activating peptide would require this ability, we investigated the binding of the designed peptides to TPR constructs incorporating the conserved LFP-acidic region, KLC1$^{extTPR}$ and KLC2$^{extTPR}$ (Figs. 2c,d).

First, the designed peptides all had improved affinities over the natural sequences. KinTag bound to KLC1$^{extTPR}$ with $K_D$ = 170 nM, which is a 13- to 44-fold increase over the parent peptides (Table 1). Moreover, and importantly, the affinities of the designed peptides for KLC$^{extTPR}$ were all reduced compared to those for KLC$^{TPR}$. This demonstrates the sensitivity of these synthetic adaptor peptides to the presence of the LFP autoinhibitory motif, which we attribute to the W-acidic component of KinTag. In turn, we anticipate that these *de novo* cargo-adaptor peptides should retain the capacity to engage the LFP-acidic activation switch.

**The X-ray crystal structure of the KLC1$^{TPR}$:KinTag complex reveals interactions as designed**

To validate our mash-up design approach, we solved the X-ray crystal structure of the KLC1$^{TPR}$: KinTag complex at the 2.85 Å resolution (Fig. 3 and Supplementary Table 2). In the crystallographic asymmetric unit, we found six copies of the KLC1$^{TPR}$: KinTag complex arranged in three independent head-to-tail dimers (Supplemtary Fig. 2). The KinTag core sequence, VFTTEDIYEWDDS, is well defined in all complexes while the *N*-terminal glycine-threonine and the *C*-terminal alanine-isoleucine dipeptides are more flexible and partly visible only in some of the molecules. As designed, the KinTag peptide binds in an extended conformation within the concave groove of the TPR

domain (Fig. 3a) with an interface area of 950 Å$^2$. This represents an increase of approximately 24% compared to SKIP W-acidic (769 Å$^2$) and of 7% over the rather extensive Torsin A Y-acidic interface (885 Å$^2$). A number of hydrogen bonds and salt bridges stabilise the peptide within the concave KLC$^{TPR}$ surface together with electrostatic complementarity between the negatively charged peptide and its receptor (Fig. 3b, Supplementary Fig. 3). While all amino acids of KinTag contribute to the interface with KLC1$^{TPR}$, it is the aromatic (F, Y, and W) residues that appear to play the key roles with 70%, 88%, and 80% of their accessible surfaces buried, respectively.

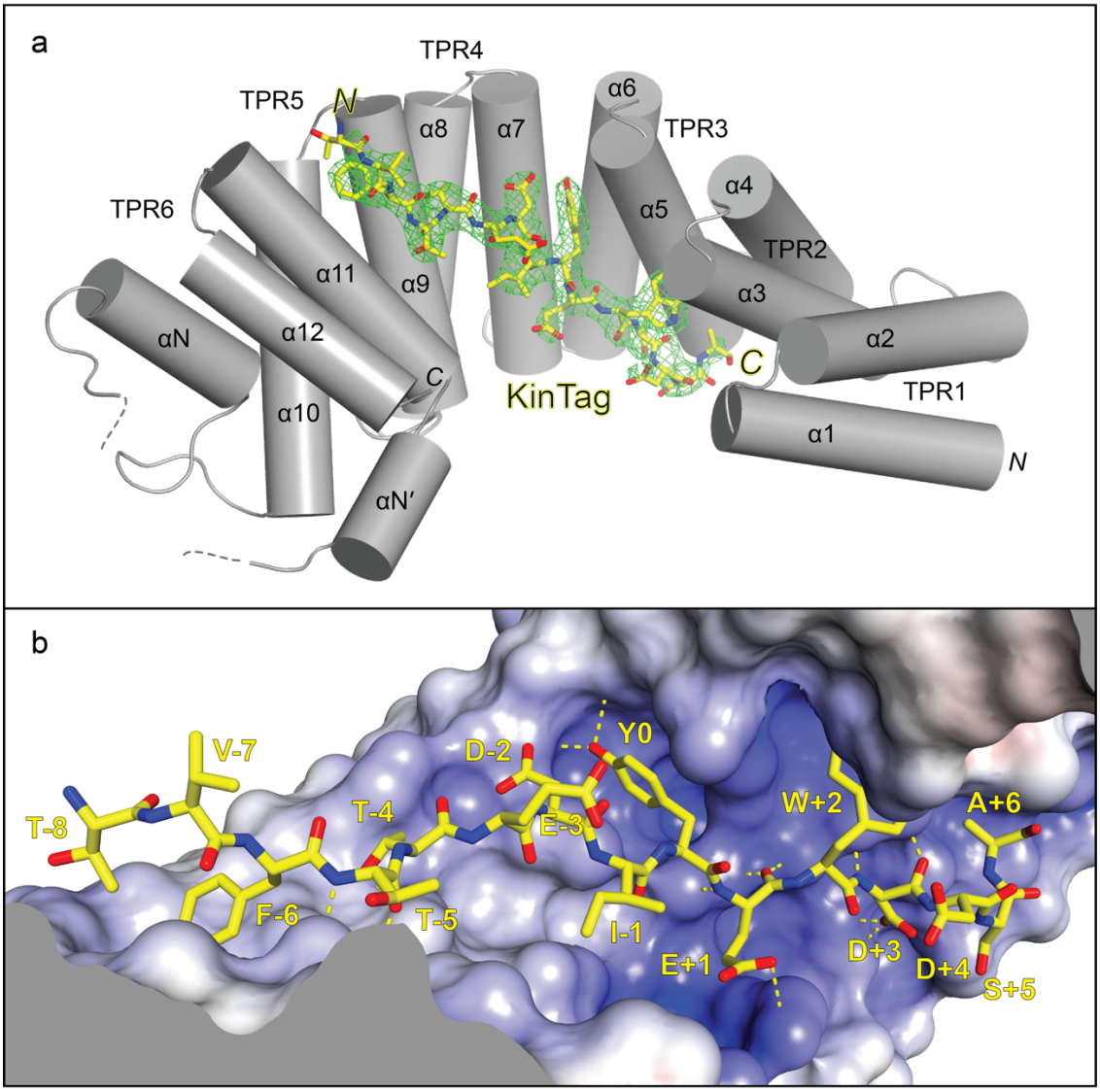

**Fig. 3 | X-ray crystal structure of the KLC1$^{TPR}$:KinTag complex. (a)** Illustrated representation of the synthetic KinTag peptide (displayed as a yellow stick model accompanied by its $2mF_o$-$DF_c$ electron density in green contoured at the 1.0 $\sigma$ level) bound to KLC1$^{TPR}$. Helices α1 to α12 of the six TPR helix-turn-helix motifs are labelled. In addition to the non-TPR helix (αN) seen in previous structures another short helix (αN') is revealed before α11. The flexible region between αN and αN' is indicated with a broken line while the engineered disordered linker connecting α12 to the KinTag is not shown for clarity. Colour-coded *N* and *C* labels indicate the *N* and *C* termini, respectively. Nitrogen and oxygen atoms are colored dark blue and red, respectively. **(b)** Sliced-surface view of KLC1$^{TPR}$ with bound KinTag. The molecular surface is coloured according to its electrostatic potential with positive and negative potential in the +10$k_B$T/e to -10$k_B$T/e range shown in blue and red, respectively. Ordered KinTag residues are numbered with the central tyrosine residue as reference. Hydrogen bonds and salt bridges are shown as broken yellow lines.

## KinTag efficiently hijacks intracellular transport

To validate the KinTag design functionally, we tested its capacity to hijack endogenous kinesin-1 to effect organelle transport in cells. Fusion proteins comprising the lysosome-associated membrane protein (LAMP1) and the green fluorescent protein (mGFP) with and without an intervening KinTag were transiently expressed in HeLa cells. A construct with the natural SKIP W-acidic sequence in place of KinTag was used as a control.[21] As expected, the control LAMP1-mGFP fusion incorporated into lysosomes, and mostly clustered in the juxtanuclear region with some dispersed through the cytoplasm (Figs. 4a-c).[36] Consistent with some limited capacity to promote transport, the single SKIP W-acidic sequence promoted measurable dispersion of lysosomes towards the cell periphery as shown by cumulative LAMP intensity (described in detail in[18,37]). By contrast, KinTag promoted a dramatic dispersion of lysosomes with prominent accumulation of the fusion proteins at cell vertices. Notably, the extent of peripheral transport correlated with the binding affinities measured *in vitro,* with the high-affinity binder effecting a greater degree of lysosome dispersion (Figs. 4a-c).

Finally, we tested if KinTag could direct the transport of lysosomes into axons. Rat primary hippocampal neurons were transfected with plasmids encoding LAMP1-

mGFP, LAMP1-SKIP-mGFP and LAMP1-KinTag-mGFP fusion proteins. Entry of lysosomes into the axon was monitored by staining for ankryin G (an axon initial segment (AIS) marker) and quantified by measurement of the ratios of mean GFP fluorescence intensity in the AIS vs soma (Figs. 4d-f). Consistent with lysosome dispersion analysis in HeLa cells, KinTag promoted the robust transport of lysosomes into the axon (Figs. 4d-f). The SKIP W-acidic sequence was not as effective. For the first time, this demonstrates that the extent of kinesin-1-dependent axonal transport is positively correlated with the *in vitro* binding affinity of the interaction between a cargo adaptor peptide and the motor complex. This adds to examples of *in vitro* properties of *de novo* designed peptides translating to *in vivo* functions.[38,39] For the case described herein, it illustrates that *mash-up* design can deliver peptides that bind their targets with high affinity *in vitro*, and operate in cells to out-perform natural adaptor sequences and increase kinesin-1-dependent transport of a chosen cargo.

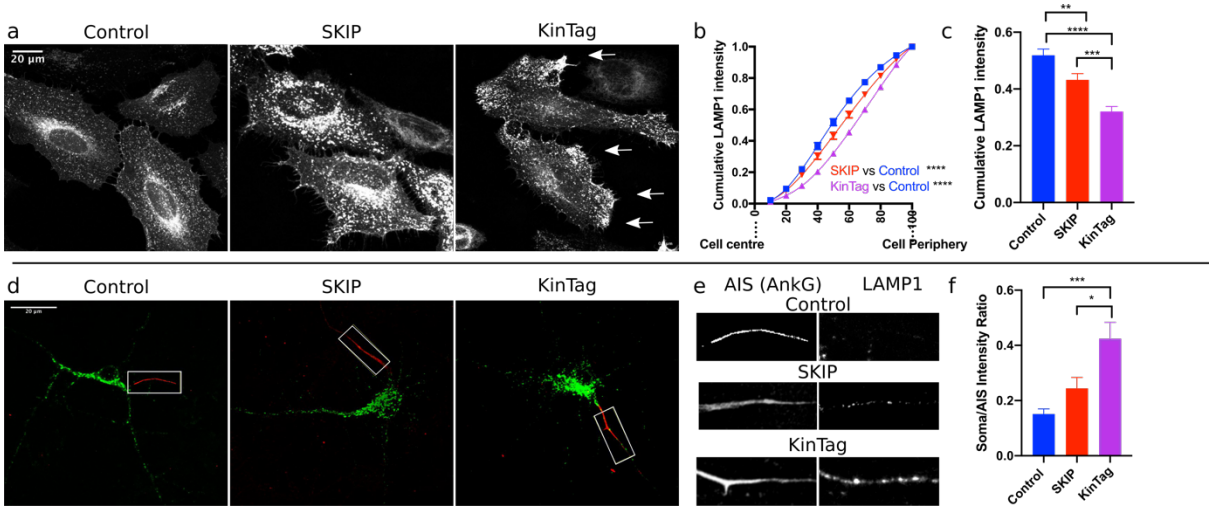


**Fig. 4 | KinTag promotes more efficient lysosome transport than the natural W-acidic sequence.** **(a)** Representative confocal fluorescence images of lysosome distribution in LAMP1-mGFP (control), LAMP1-SKIP-mGFP (SKIP) and LAMP1-KinTag-mGFP (KinTag) transfected HeLa cells. Scale bar is 20 µM. **(b)** Quantification of lysosome distribution by measuring cumulative fluorescence intensity from cell centre to cell periphery a minimum of 25 cells from 3 independent experiments. Fitted curves are compared using the extra sum of F-squares test (**c**) Comparision of cumulative LAMP1 intensity at the 50$^{th}$ percentile. Error bars show S.E.M. and unpaired T-test is used for statistical analysis. **(d)** Representative confocal fluorescence images of lysosome distribution in LAMP1-mGFP (control), LAMP1-SKIP-mGFP (SKIP) and LAMP1-KinTag-mGFP (KinTag) in primary hippocampal neurons. **(e)** Split-channel magnified images of boxed regions from **d** showing the axonal initial segment (AIS) marked by Ankryn-G (AnkG). **(f)** Quantification of ratio of fluorescence intensity in the soma and AIS

in transfected neurons in a minimum of 12 cells from 3 independent experiments. Error bars show S.E.M. and unpaired T-test is used for statistical analysis. * P< 0.05, ** P< 0.01, *** P<0.001, **** P < 0.0001.

## Discussion

The recognition of client-peptide motifs by protein machineries is a ubiquitous feature of the dynamic cell. It enables different clients (*e.g.*, integral membrane proteins) to be selected by conserved machineries (*e.g.*, molecular motors or vesicle coats) to ensure the clients are directed to appropriate sites for their function, recycling, or degradation.[17,40] Here we show that this can be manipulated by design.

We employ a novel *mash-up* design approach to link binding features from natural sequences into a single, high-affinity peptide, KinTag, to hijack kinesin-1 dependent microtubule transport. At a molecular level, our design approach is validated by X-ray crystallography, and its functional utility is demonstrated in lysosome transport assays. For the first time, this reveals that peptide-protein binding affinities measured *in vitro* correlate with the extent of cargo transport in the cell. Our study opens the door to manipulating similar interactions throughout transport and trafficking networks, where similar unitarily low affinity natural interactions are typically supported through co-operativity, avidity and coincidence detection, and thus may be amenable to augmentation through the design of high-affinity peptide ligands.

More broadly, *mash-up* design provides a strategy for developing high-affinity peptide ligands for protein surfaces. The structure of the KLC1$^{TPR}$:KinTag complex confirms that both general design features (*i.e.*, shape and charge complementarity between the peptide and the protein) and sequence-specific design features (*i.e.*, large side chains of the peptide bind into designated pockets of the protein) are realized. This highlights the utility of fragment linking in peptide design, akin to that used with small-molecule pharmacophores.[33,34] Crucially, we have been able to incorporate a

key function of a natural ligand—namely, operating the KLC autoinhibitory switch—[22,27] demonstrating that complex functionality can be retained from peptide fragments.

Finally, our data reinforce the key role and intrinsic sufficiency of TPR groove binding peptides for motor recruitment and activation. Through comparison of *in vitro* measured binding affinities with the extent of cargo transport, we have demonstrated, for the first time, that these are positively correlated. These findings should allow a toolkit of peptide ligands, across a range of affinities, to be developed as transport tags within cells. This will allow investigation of the relationship between *in vitro* binding affinity and binding kinetics, with the cellular mechanics of vesicle and organelle transport. In turn, we envisage the orchestration of transport of organelles, and other cargoes, to investigate the functional roles of positioning within the cell. It is conceivable that the design of relatively low molecular weight, high-affinity, peptide ligands for kinesin-1 could be useful in the spatial (*e.g.*, axon specific) targeting of exogenous therapeutic cargoes for the treatment of neurological disease.

## ACKNOWLEDGEMENTS

J.A.C is supported by the EPSRC Bristol Centre for Doctoral Training in Chemical Synthesis. M.P.D. is a Lister Institute for Preventative Medicine Research Prize Fellow and work in his lab is supported by BBSRC grant BB/S000917/1. D.N.W. held a Royal Society Wolfson Research Merit Award (WM140008). M.S.C. and R.A.S. are supported by BBSRC grant BB/S000828/1. We also thank the University of Bristol School of Chemistry Mass Spectrometry Facility for use of the EPSRC-funded Bruker Ultraflex MALDI-TOF/TOF instrument (EP/K03927X/1), and the BBSRC/EPSRC-funded BrisSynBio (BB/L01386X1) for access to its peptide synthesizers and plate reader. The X-ray crystallographic work was conducted at beamline I03 of Diamond

Light Source. The authors also thank Kirsty McMillan for donation of rat hippocampal neurons and antibodies and assistance with experimental protocols.

## AUTHOR CONTRIBUTION

M.P.D., D.N.W and J.A.C. conceived the project and designed the peptides. J.A.C. synthesised the peptides and completed biophysical and cellular experiments. R.A.S. and M.S.C. designed the construct used for crystallographic studies and solved the X-ray crystal structure of the complex. The manuscript was written by J.A.C., M.P.D., D.N.W. and R.A.S. and commented on by all authors.

## COMPETING INTERESTS STATEMENT

The authors declare no competing interests.

## REFERENCES

1 Neduva, V. *et al.* Systematic discovery of new recognition peptides mediating protein interaction networks. *PLoS biology* **3**, e405, (2005).
2 London, N., Raveh B Fau - Schueler-Furman, O. & Schueler-Furman, O. Druggable protein-protein interactions--from hot spots to hot segments. *Curr. Opin. Cell. Biol.* **17**, 952-959 (2013).
3 Reichen, C., Hansen, S. & Pluckthun, A. Modular peptide binding: from a comparison of natural binders to designed armadillo repeat proteins. *J. Struct. Biol.* **185**, 147-162 (2014).
4 Perez-Riba, A. & Itzhaki, L. S. The tetratricopeptide-repeat motif is a versatile platform that enables diverse modes of molecular recognition. *Curr. Opin. Struc. Biol.* **54**, 43-49 (2019).
5 Grove, T. Z., Cortajarena, A. L. & Regan, L. Ligand binding by repeat proteins: natural and designed. *Curr. Opin. Struc. Biol.* **18**, 507-515 (2008).
6 D'Andrea, L. D. & Regan, L. TPR proteins: the versatile helix. *Trends Biochem. Sci.* **28**, 655-662 (2003).
7 Main, E. R., Lowe, A. R., Mochrie, S. G., Jackson, S. E. & Regan, L. A recurring theme in protein engineering: the design, stability and folding of repeat proteins. *Curr. Opin. Struc. Biol.* **15**, 464-471 (2005).
8 Randall, T. S. *et al.* A small-molecule activator of kinesin-1 drives remodeling of the microtubule network. *Proc. Natl. Acad. Sci. USA* **114**, 13738-13743 (2017).
9 Binz, H. K. *et al.* High-affinity binders selected from designed ankyrin repeat protein libraries. *Nat. Biotechnol.* **22**, 575-582 (2004).

10 Dodding, M. P., Mitter, R., Humphries, A. C. & Way, M. A kinesin-1 binding motif in vaccinia virus that is widespread throughout the human genome. *EMBO J.* **30**, 4523-4538 (2011).
11 Boucrot, E., Henry, T., Borg, J. P., Gorvel, J. P. & Meresse, S. The intracellular fate of Salmonella depends on the recruitment of kinesin. *Science* **308**, 1174-1178 (2005).
12 Hirokawa, N., Niwa, S. & Tanaka, Y. Molecular motors in neurons: transport mechanisms and roles in brain function, development, and disease. *Neuron* **68**, 610-638 (2010).
13 Hirokawa, N., Noda, Y., Tanaka, Y. & Niwa, S. Kinesin superfamily motor proteins and intracellular transport. *Nature reviews. Mol. Cell. Biol.* **10**, 682-696 (2009).
14 Vale, R. D., Reese, T. S. & Sheetz, M. P. Identification of a novel force-generating protein, kinesin, involved in microtubule-based motility. *Cell* **42**, 39-50 (1985).
15 Pernigo, S., Lamprecht, A., Steiner, R. A. & Dodding, M. P. Structural basis for kinesin-1:cargo recognition. *Science***340**, 356-359 (2013).
16 Pernigo, S. *et al.* Structural basis for isoform-specific kinesin-1 recognition of Y-acidic cargo adaptors. *eLife* **7**, e38362 (2018).
17 Cross, J. A. & Dodding, M. P. Motor-cargo adaptors at the organelle-cytoskeleton interface. *Curr. Opin. Cell. Biol.* **59**, 16-23 (2019).
18 Sanger, A. *et al.* SKIP controls lysosome positioning using a composite kinesin-1 heavy and light chain-binding domain. *J. Cell. Sci.* **130**, 1637-1651 (2017).
19 Blasius, T. L., Cai, D., Jih, G. T., Toret, C. P. & Verhey, K. J. Two binding partners cooperate to activate the molecular motor Kinesin-1. *J. Cell. Sci.* **176**, 11-17 (2007).
20 Fu, M.-m. & Holzbaur, E. L. F. JIP1 regulates the directionality of APP axonal transport by coordinating kinesin and dynein motors. *J. Cell. Sci.* **202**, 495-508 (2013).
21 Pu, J. *et al.* BORC, a multisubunit complex that regulates lysosome positioning. *Dev. Cell.* **33**, 176-188 (2015).
22 Yip, Y. Y. *et al.* The light chains of kinesin-1 are autoinhibited. *Proc. Natl. Acad. Sci. USA* **113**, 2418-2423 (2016).
23 Hackney, D. D. & Stock, M. F. Kinesin's IAK tail domain inhibits initial microtubule-stimulated ADP release. *Nat. Cell. Biol.* **2**, 257-260 (2000).
24 Kaan, H. Y., Hackney, D. D. & Kozielski, F. The structure of the kinesin-1 motor-tail complex reveals the mechanism of autoinhibition. *Science* **333**, 883-885 (2011).
25 Dietrich, K. A. *et al.* The kinesin-1 motor protein is regulated by a direct interaction of its head and tail. *Proc. Natl. Acad. Sci. USA* **105**, 8938-8943 (2008).
26 Farías, G. G., Guardia, C. M., De Pace, R., Britt, D. J. & Bonifacino, J. S. BORC/kinesin-1 ensemble drives polarized transport of lysosomes into the axon. *Proc. Natl. Acad. Sci. USA* **114**, E2955-E2964 (2017).
27 Kawano, T. *et al.* A Small Peptide Sequence is Sufficient for Initiating Kinesin-1 Activation Through Part of TPR Region of KLC1. *Traffic* **13**, 834-848 (2012).
28 London, N., Raveh, B. & Schueler-Furman, O. Peptide docking and structure-based characterization of peptide binding: from knowledge to know-how. *Curr. Opin. Struc. Biol.* **23**, 894-902 (2013).
29 Modell, A. E., Blosser, S. L. & Arora, P. S. Systematic Targeting of Protein-Protein Interactions. *Trends Pharmacol. Sci.* **37**, 702-713 (2016).

30 Hansen, S., Kiefer, J. D., Madhurantakam, C., Mittl, P. R. E. & Plückthun, A. Structures of designed armadillo repeat proteins binding to peptides fused to globular domains. *Protein Sci.* **26**, 1942-1952 (2017).
31 Forrer, P., Binz, H. K., Stumpp, M. T. & Plückthun, A. Consensus design of repeat proteins. *Chembiochem* **5**, 183-189 (2004).
32 Kajander, T., Cortajarena, A. L. & Regan, L. Consensus design as a tool for engineering repeat proteins. *Methods Mol. Biol.* **340**, 151-170 (2006).
33 Erlanson, D. A. Introduction to fragment-based drug discovery. *Topics Curr. Chem.* **317**, 1-32 (2012).
34 Hall, D. R., Kozakov, D., Whitty, A. & Vajda, S. Lessons from Hot Spot Analysis for Fragment-Based Drug Discovery. *Trends Pharmacol. Sci.* **36**, 724-736 (2015).
35 Verhey, K. J. *et al.* Cargo of Kinesin Identified as Jip Scaffolding Proteins and Associated Signaling Molecules. *J. Cell. Biol.* **152**, 959-970 (2001).
36 Falcón-Pérez, J. M., Nazarian, R., Sabatti, C. & Dell'Angelica, E. C. Distribution and dynamics of Lamp1-containing endocytic organelles in fibroblasts deficient in BLOC-3. *J. Cell. Sci.* **118**, 5243-5255 (2005).
37 Starling, G. P. *et al.* Folliculin directs the formation of a Rab34-RILP complex to control the nutrient-dependent dynamic distribution of lysosomes. *EMBO Rep.* **17**, 823-841 (2016).
38 Smith, A. J., Thomas, F., Shoemark, D., Woolfson, D. N. & Savery, N. J. Guiding Biomolecular Interactions in Cells Using de Novo Protein-Protein Interfaces. *ACS Synth. Biol.* **8**, 1284-1293 (2019).
39 Ljubetič, A. *et al.* Design of coiled-coil protein-origami cages that self-assemble in vitro and in vivo. *Nat. Biotechnol.* **35** (2017).